Discrete and Differential Two-View Constraints for General Imaging Systems

Robert Pless
Washington University in St. Louis
Box 1045, One Brookings Ave, St. Louis, MO, 63130
pless@cs.wustl.edu

Abstract

The recent popularity of catadioptic and multi-camera imaging systems indicates a need to create formal models for general, non-perspective camera geometries. Development of algorithmic tools for interpreting images from a generalized camera model will lead to a better understanding of how to design camera systems for particular tasks. Here we define the corollary to epi-polar constraints for standard cameras — the relationship between two images of a scene taken by generalized cameras from viewpoints related by discrete or differential motions.

1 Introduction

The geometric relationships between several images taken of the same scene from different viewpoints has been the central subject of study in the Computer Vision community for many years [4, 9]. The relationships have been formalized for orthographic, affine, and perspective projections. Recently, new camera designs have appeared with many different imaging geometries (a very good compilation is [2]). For many purposes, these non-standard camera systems have significant advantages over pinhole or orthographic cameras.

The description and analysis of non-central projection camera systems ranges from very general imaging systems to those whose imaging geometry is highly constrained. The most general case allows an arbitrary mapping between image pixels and the part of the scene imaged by that pixel. This has been studied in the context of generating these images [15], and calibrating this imaging device [7]. More specialized camera geometries include linear push-broom cameras [8] and stereo panoramic cameras [13]. The equations of motion have been studied for a number of specific non-standard camera systems, including estimating optic flow from multi-camera systems [1, 3], and catadioptic systems [6].

Since new camera designs are constantly being proposed, it is useful to define a general framework for the analysis of non-central projection cameras which encompasses all new camera designs. The introduction and analysis of the oblique camera model [12] is one step in this direction, as it subsumes several of the existing non-standard camera models, including the linear push-broom and the stereo panoramic cameras. The oblique camera model considers camera geometries where a point in the world is imaged at most once by the camera — a system where none of the rays that are captured intersect.

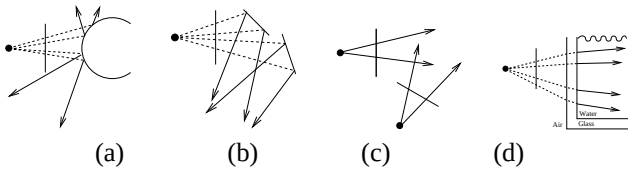

(a) (b) (c) (d)

Figure 1. Examples of camera capturing systems within the framework of this paper. (a) A catadioptic system consisting of a camera looking at a curved mirror. (b) An imaging system created with multiple flat mirrors. (c) A rigidly mounted system of multiple synchronized cameras. (d) A scene being viewed through an optical interface which refracts the visible light. Note that the lines captured by these camera systems do not all pass through a single point (a non-central-projection).

In this work we remove all restrictions on the camera model, and provide an analysis of the geometry relating two views from the most generalized camera model, as considered by [15, 7]. This camera model encompasses all of the imaging situations depicted in Figure 1 – multiple-camera systems, catadioptic imaging systems and cameras which view a scene through an optical interface. The only requirement is that there exists a one to one mapping between image pixels and the ray in space along which that pixel views. There are no constraints on the projection model. In

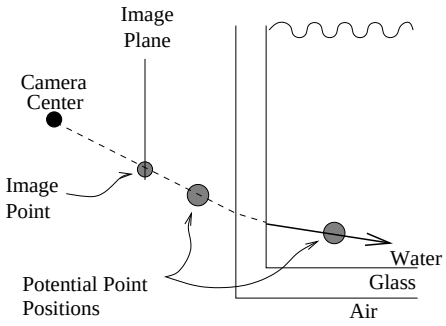

Figure 2. Environments without a one to one mapping between pixel coordinates and scene rays are imaging systems not included in this framework. For instance, from figure 1d, if an object can appear either before or after the optical interface, it is not known which line the pixel is sampling. Only if the system is used so that all visible objects are in the water would this case follow the framework in this model.

fact, the analysis does not even require an explicit projection model – the geometric constraints rely only on the inverse projection model, a mapping from image pixels to rays in the scene. This mapping can be defined as a function of the image coordinates, or simply a list, explicitly defining, for each pixel, which ray in space it samples.

This mapping, from image pixel to scene ray, must remain the same from frame to frame. Consider the imaging system shown in Figure 1 b — a rigid motion of this camera system includes a rigid motion of *both* the camera and the mirrors. Relative to the camera coordinate system, the set of rays sampled by the camera is always the same. Furthermore, the pixel to scene ray mapping must be one to one. For systems which include rays which reflect or refract, the analysis only applies if the camera is used in such a way that objects appear along a specific ray segment. Using a camera systems such as the one depicted in Figure 2 — when objects may appear either before or after the ray refracts — does not fit within this framework.

Calibrating this imaging system is significantly more difficult than calibrating a pinhole camera system. Also, many assumptions that are valid for normal camera geometries may not be valid for the arbitrary sensor geometries captured within this general framework. There may be discontinuities in the image capture process. Sampling issues which may be safely ignored for normal cameras may cause problems in the image analysis from general cameras. Standard feature detectors may fail because different parts of the image may have very different sampling properties. Classifying situations when sampling issues present problems needs to be considered on an application specific basis. This work is intended only to consider the geometric relationships, and to provide a general framework for the analysis of new camera designs.

The following section describes some necessary background on the definition and calibration of the general imaging model. Then the relationships between two views of a static scene are illustrated, first for the case of the camera undergoing a discrete motion, in Section 3, and then for the case of differential motion, in Section 4. Section 5 gives two examples of real imaging systems considered in this generalized model; the discrete motion of a camera looking through an optical interface, and discrete and differential measurements from the bizarre eye of a stomatopod.

2 General Imaging Model

The general imaging model abstracts away from exactly what path light takes as it passes through the lenses and mirrors of an arbitrary imaging system. Instead, it identifies each image sensor reading with the region of space that affects that sensor. A reasonable model of this region of space is a cone emanating from some point. A complete definition of the imaging model has been defined in terms of "raxels" [7], (see Figure 3).

A raxel includes the following information about how a particular pixel samples the scene. This sampling is assumed to be centered around a ray starting at a point X,Y,Z, with a direction parameterized by (ϕ, θ). This pixel captures light from a cone around that ray, whose aspect ratio and orientation is given by (f_a, f_b, Υ). The light intensity captured may also be attenuated, these radiometric quantities may also differ for every pixel.

For the geometric analysis of multiple images, we simplify this calibration so that it only includes the definition of the ray that the pixel samples. This gives a simpler calibration problem which requires determining, for each pixel, the Plücker vectors of the sampled line. Since Plücker vectors are required for the mathematical analysis presented later, the following section gives a brief introduction.

2.1 Plücker Vectors

In order to describe the line in space that each pixel samples in this more general camera setting, we need a mechanism to describe arbitrary lines in space. There are many parameterizations of lines, but Plücker vectors [14] give a convenient mechanism for the types of transformations that are required. The Plücker vectors of a line are a pair of 3-vectors: q, q', named the direction vector and moment vector. q is a vector of any length in the direction of the line. Then, $q' = q \times P$, for any point P on the line. There are two constraints that this pair of vectors must satisfy. First,

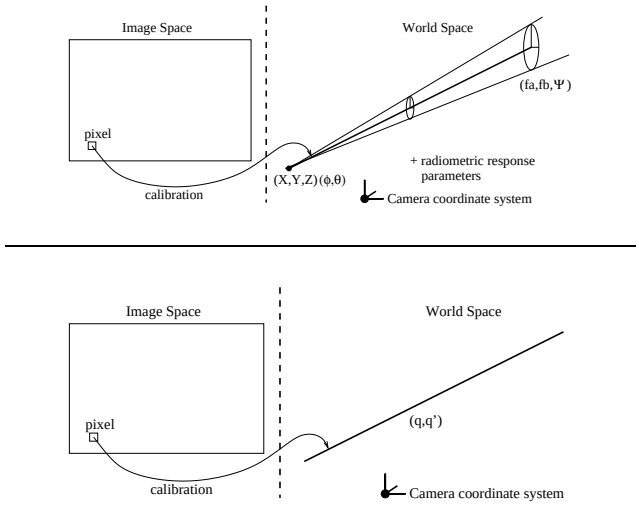

Figure 3. (Top) The generalized imaging system defined in [7] expresses, for each pixel, a description of how that pixel samples the light-field. This sampling is assumed to be centered around a ray starting at a point X,Y,Z, with a direction parameterized by (ϕ, θ), relative to a coordinate system attached to the camera. The pixel captures light from a cone around that ray, whose aspect ratio and orientation is given by (f_a, f_b, Υ). The light intensity captured may also be attenuated, these radiometric quantities may also differ for every pixel. (Bottom) The simplified imaging model parameterizes only the ray along which the scene is sampled, and does not consider radiometric properties. The ray is parameterized by its Plücker vectors q, q'.

$q \cdot q' = 0$, and second, the remaining five parameters are homogeneous, their overall scale does not affect which line they describe. It is often convenient to force the direction vector to be a unit vector, which defines a scale for the homogeneous parameters.

If q is a unit vector, the point $(q \times q')$ is the point on the line (defined by q, q') closest to the origin. The set of all points that lie on a line with these Plücker vectors is given by:

$$(q \times q') + \alpha q, \forall \alpha \in R \tag{1}$$

2.2 Plücker Calibration

The simplified calibration is an arbitrary mapping between pixel coordinates and the ray captured by that pixel. The calibration function is the mapping between each pixel captured by the camera and the line of sight captured by that pixel. This line is defined by its Plücker vectors. The calibration of this camera system defines the mapping between pixel coordinates and lines. The line captured by pixel (x, y) is $\langle q(x, y), q'(x, y) \rangle$. Most of the remainder of this paper discusses the constraint given by corresponding points in two images, or the optic flow at a point. In this case we drop the coordinates (x,y), and list the Plucker vectors simply as q, q'.

The analysis of differential camera motion is only possible if the imaging system smoothly samples the environment — that is if the ray sampled by one pixel is close to the ray sampled by neighboring pixels. This is the case for figure 1 (a). For the other camera systems, these differential quantities are not defined over discontinuities in the imaging process, such as the boundary between one mirror and another in figure 1 (b). Between these discontinuities, it is possible to define how the Plücker vectors of the sampled ray change with respect to a change of location in the image. That is to say, the following quantities are also defined (in our implementation they are estimated as differences of the q, and q' between neighboring pixels).

$$\frac{\partial q(x,y)}{\partial x}, \frac{\partial q(x,y)}{\partial y}, \frac{\partial q'(x,y)}{\partial x}, \frac{\partial q'(x,y)}{\partial y}$$

These are four vector quantities — for intuition, in a standard normalized pinhole camera, $q'(x, y)$ is uniformly zero, $\frac{\partial q(x,y)}{\partial x} = \langle 1, 0, 0 \rangle$, and $\frac{\partial q(x,y)}{\partial y} = \langle 0, 1, 0 \rangle$. The calibration for the more generalized imaging system discussed in [7] (finding all of the parameters of the raxel) suffices to define the parameters of the Plücker Calibration. Additionally, the main contribution of this work is a theoretical model which encompasses many different specialized camera geometries. For any specific such geometry, the calibration process can be simplified. Given this background, we

can now consider the relationships between multiple images captured by these generalized cameras.

3 Discrete Motion

Suppose, in two generalized images, we have a correspondence between pixel (x_1, y_1) in the first image and pixel (x_2, y_2) in a second image. In our camera system, these points are projections of a 3d point which lies along lines in space described by Plücker vectors $\langle q_1, q_1{}' \rangle$, and $\langle q_2, q_2{}' \rangle$. The camera viewpoints are related by an arbitrary rigid transformation. There is a rotation R and a translation T which takes points in the coordinate system of the first camera and transforms them into the coordinate system of the second camera.

After this rigid transformation, the Plücker vectors of the first line in the second coordinate system become:

$$\langle Rq_1, Rq_1' + R(T \times q_1) \rangle \tag{2}$$

Since we have a pair of corresponding points, this line must intersect the line defined by the pixel coordinates of the corresponding point in the second camera. A pair of lines with Plücker vectors $\langle q_a, q_a{}' \rangle$, and $\langle q_b, q_b{}' \rangle$ intersect if and only if:

$$q_b \cdot q_a' + q_b' \cdot q_a = 0. \tag{3}$$

This allows us to write down the constraint given by the correspondence of a point between two images, combining Equations 2 and 3

$$q_2 \cdot (Rq_1' + R(T \times q_1)) + q_2' R q_1 = 0.$$

This completely defines how two views of a point constrain the discrete motion of a generalized camera (using the convention that $[T]_x$ is the skew symmetric matrix such that $[T]_x v = T \times v$ for any vector v):

Generalized Epi-polar Constraint

$$q_2{}^T R q_1' + q_2^T R [T]_x q_1 + q_2'{}^T R q_1 = 0. \tag{4}$$

For standard perspective projection cameras, $q_1' = q_2' = 0$, and what remains: $q_2^T R [T]_x q_1 = 0$, is the classical epi-polar constraint defined by the Essential matrix. Strictly speaking, this is not exactly analogous to the epi-polar constraint for standard cameras. For a given point in one image, the above equation may have none, one, several, or an infinite number of solutions depending on what the exact camera geometry is. The name generalized epi-polar constraint, however, is fitting bvecause it describes how two corresponding points constrain the relative camera motions.

Given the camera transformation R, T and corresponding points, it is possible to determine the 3D coordinates of the world point in view. Using Equation 1, and transforming the first line into the second coordinate system, solving for the position of the point in space amounts to finding the intersection of the corresponding rays. This requires solving for the parameters α_1, α_2, which is the corollary of the depth in typical cameras:

$$R((q_1 \times q_1') + \alpha_1 q_1) + T = (q_2 \times q_2') + \alpha_2 q_2$$

Collecting terms leads to the following vector equation whose solution allows the reconstruction of scene point P in the coordinate system of the first camera.

Generalized Point Reconstruction

$$\alpha_1 R q_1 - \alpha_2 q_2 = (q_2 \times q_2') - R(q_1 \times q_1') - T,$$

solve above equation for α_1, and use below

$$P = q_1 \times q_1' + \alpha_1 q_1$$

4 Differential Motion

In the differential case, we will consider the image of a point P in space which is moving with a translation velocity $\vec{t}$, and an angular velocity, (relative to origin of the camera coordinate system) $\vec{\omega}$. The instantaneous velocity of the 3D point is:

$$\dot{P} = \vec{\omega} \times P + \vec{t}.$$

For a point in space to lie on a line with Plücker vectors $\langle q, q' \rangle$, the following must hold true:

$$P \times q - q' = \vec{0};$$

As the point moves, the Plücker vectors of the lines incident upon that point change. Together, the motion of the point and the change in the Plücker vectors of the line incident on that point must obey:

$$\frac{\partial}{dt}(P \times q - q') = \vec{0}, \text{or},$$
$$\dot{P} \times q + P \times \dot{q} - \dot{q}' = 0$$

In terms of the parameters of motion, this gives:

$$(\vec{\omega} \times P + \vec{t}) \times q + P \times \dot{q} - \dot{q}' = \vec{0}.$$
$$(\vec{\omega} \times P + \vec{t}) \times q = \dot{q}' - P \times \dot{q}. \tag{5}$$

Which are constraints relating the camera motion and the line coordinates incident on a point in 3D for a particular rigid motion. On the image plane, the image of this point is undergoing a motion characterized by its optic flow, (u, v) on the image plane. Combining this optic flow with the camera calibration, one can calculate how the coordinates of the Plücker vectors must be changing:

$$\begin{aligned} \dot{q} &= \frac{\partial q}{\partial x}u + \frac{\partial q}{\partial y}v, \\ \dot{q}' &= \frac{\partial q'}{\partial x}u + \frac{\partial q'}{\partial y}v, \end{aligned} \tag{6}$$

so that we can consider $\dot{q}$ and $\dot{q}'$ to be image measurements. Then we can substitute Equation 1 into Equation 5 to get:

$$(\vec{\omega} \times ((q \times q') + \alpha q) + \vec{t}) \times q = \dot{q}' - ((q \times q') + \alpha q) \times \dot{q}.$$

or,

$$(\vec{\omega}\times(q\times q'))\times q+\alpha(\vec{\omega}\times q)\times q+\vec{t}\times q = \dot{q}'-(q\times q')\times\dot{q}+\alpha q\times\dot{q}. \tag{7}$$

The following identities hold when $|q| = 1$,

$$\begin{aligned} (\vec{\omega} \times (q \times q')) \times q &= (\vec{\omega} \cdot q)(q \times q'), \text{ and,} \\ (\vec{\omega} \times q) \times q) &= (\vec{\omega} \cdot q)q - \vec{\omega}, \\ (q \times q') \times \dot{q} &= -(q' \cdot \dot{q})q, \end{aligned}$$

Simplifying Equation 7 and collecting terms gives:

$$\alpha((\vec{\omega}\cdot q)q-\vec{\omega}-q\times\dot{q})+\vec{t}\times q = \dot{q}'+(q'\cdot\dot{q})q-(\vec{\omega}\cdot q)(q\times q') \tag{8}$$

This vector equation can be simplified by taking the cross product of each side with the vector q, which gives:

$$\alpha(\vec{\omega} \times q) + (\vec{t} \times q) \times q = \dot{q}' \times q + (\vec{\omega} \cdot q)q' + \alpha\dot{q}.$$

Collecting the terms that relate to the distance of the point along the sampled ray, then dividing by α gives:

$$(\vec{\omega} \times q - \dot{q}) = \frac{-(\vec{t} \times q) \times q + \dot{q}' \times q + (\vec{\omega} \cdot q)q'}{\alpha}$$

which can be written more cleanly to define the optic flow for a generalized camera under differential motion:

Generalized Optic Flow Equation

$$\dot{q} = \vec{\omega} \times q + \frac{(\vec{t} \times q) \times q - \dot{q}' \times q - (\vec{\omega} \cdot q)q'}{\alpha} \tag{9}$$

For standard perspective projection cameras, $q' = 0$, and $\dot{q}' = 0$, and this simplifies to the standard optic flow equation (for spherical cameras):

$$\dot{q} = (\vec{\omega} \times q) + \frac{(\vec{t} \times q) \times q}{\alpha}$$

On approach to finding the camera motion starts by finding an expression relating the optic flow to the motion parameters that is independent of the depth of the point. This differential form of the epi-polar constraint is:

$$\dot{q} \times ((\vec{t} \times q) \times q) = (\vec{\omega} \times q) \times ((\vec{t} \times q) \times q).$$

This same process can be applied to generalized cameras, giving:

Generalized Differential Epi-polar Constraint

$$(\dot{q}-\vec{\omega}\times q)\times((\vec{t}\times q)\times q-\dot{q}'\times q-(\vec{\omega}\cdot q)q') = 0, \tag{10}$$

which, like the formulation for planar and spherical cameras, is bilinear in the translation and the rotation and independent of the depth of the point.

5 Discussion

In this section we illustrate the two view geometry for two different imaging systems that fall in the generalized camera model. The first involves a camera looking through an optical interface, the second considers the eye of a shrimp (stomatopod). Each of these imaging systems is a non-central projection.

5.1 Vision through optical interfaces

Many visual measurement processes, especially measurement tasks in various physical sciences, require a camera to view a scene of interest through an optical interface. Light refracts as it passes through an optical interface, so the standard pinhole model does not model the set of rays, in the scene of interest, that the camera is capturing.

The calibration of a view through an optical interface is highly application dependent. As an example application we considered a camera that is imaging a lava lamp (an toy consisting of a glass jar with colored wax and water which is heated from below. The heat causes globules of wax to rise — where they cool and subsequently sink). The standard intrinsic camera calibration was calculated from many images

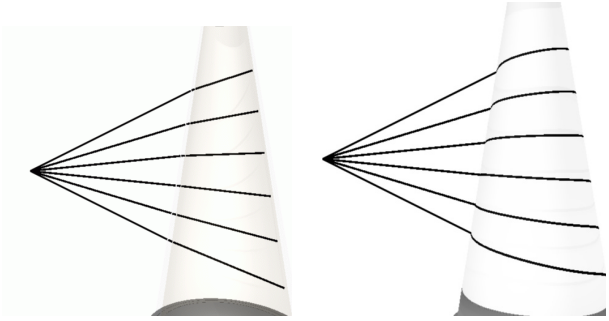

Figure 4. An illustration of light ray distortion at an optic interface. Left: A view of the rays imaged by the camera on the left and how they are refracted at the optical interface. Right: The view of those rays from a second camera is also distorted by the optical interface.

of a planar checkerboard pattern [16]. This checkerboard was then augmented with a rigidly attached arm with identifiable points (a narrow checkerboard). An image of the checkerboard with a standard, calibrated camera allowed for the solution of the 3D position of the augmenting arm. Eight thousand images of this form were taken, and the image position of the points on the augmenting arm, were captured with the 3D position of the arm. This was sufficient so that 17% of the pixels imaging the lava lamp had 2 or more samples of 3D points, sufficient to define the ray in the lava lamp along which they view. The calibration data was interpolated to extend to the remaining pixels which did not capture multiple 3D points in the calibration data set.

The calibration data was used to create a simulated views of the lava lamp. Figure 6 shows two views of the lava lamp, a dark point in the center of the left view and the corresponding epi-polar curve in the right image.

5.2 Analysis of biological vision systems

Biological vision systems exhibit an astonishing diversity of design and function. Many mammals have eyes that are similar to standard video cameras, so pinhole camera model is a reasonable model for the imaging process. Insects, on the other the hand, tend to have more panoramic vision. For some insects this is relatively close to a central projection and the eye approximates the mathematical form of a spherical camera. For other systems, however, the view cannot be modeled by any central projection. One example of this is the astounding eye of the stomatopod 7.

The set of rays captured by the stomatopod eye was estimated from published goniometer measurements [10]. The strip along the middle of the eye is known to have 16 visual pigments (as opposed to human eyes, which have 3). One

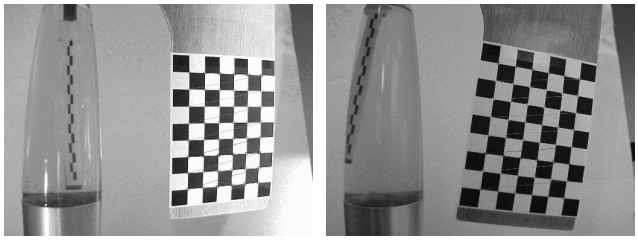

Figure 5. Two of the calibration images used to solve for the mapping from image pixels to rays *inside* the lava lamp, through the optical interface. A checkerboard with a rigidly attached "arm" with identifiable points is used. The 3D position of the checkerboard is determined from its image in a calibrated (normal, not generalized) camera, this defines the 3D position of the arm that is inside the lava lamp.

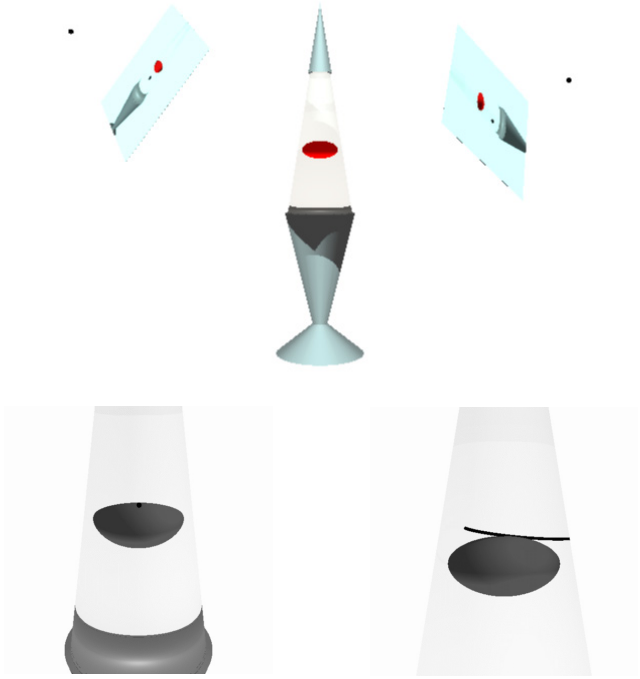

Figure 6. Two artificially generated views of the lava lamp, with the epi-polar geometry shown in the bottom images. Without an explicit projection model it is necessary to search through the rays in the (bottom right) image to find those that (nearly) intersect with the ray captured by the dark point in the (bottom left) image.

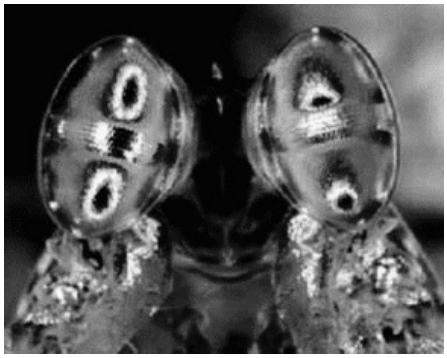

Figure 7. The compound eyes of stomatopods are on independently movable stalks. Each eye has three regions, two roughly hemispherical outer regions, separated by a roughly cylindrical strip between them which has up to 16 visual pigments. This image, taken directly of the stomatopod eye, illustrates the eye geometry. The reflection of the dark camera and white background is visible three times in left eye, and twice in the right, because multiple different parts of each eye image the region of space occupied by the camera (figure used with permision, from [10].

theory on the formation of this eye is that the two hemispherical regions are optimized to estimate the eye rotation. As the eye rotates, the thin strip samples different parts of the visual field to paint or mosaic a high (color) resolution image of the environment. This is supported by reports of the natural motion of the shrimp eye which appears as a continual slow random scanning motion. This is an example of the natural world evolving non-standard image systems for particular tasks. Although it appears that data from all three regions may not be used to compute motion in this biological system, the equations given in Sections 3 and 4 would allow the analysis of two views separated by either discrete or differential motion of this eye.

References

[1] Patrick Baker, Robert Pless, Cornelia Fermuller, and Yiannis Aloimonos. New eyes for shape and motion estimation. In *Biologically Motivated Computer Vision (BMCV2000)*, 2000.

[2] Ryad Benosman and Sing Bing Kang, editors. *Panoramic Vision: Sensors, Theory, Applications*. Springer-Verlag, 2001.

[3] Atsushi Chaen, Kazumasa Yamamzawa, Naokazu Yokoya, and Haruo Takemura. Acquisition of three-dimensional information using omnidirectional stereo vision. In *Asian Conference on Computer Vision*, volume I, pages 288–295, 1998.

[4] Olivier Faugeras. *Three-Dimensional Computer Vision*. MIT Press, Cambridge, MA, 1993.

[5] C. Fermüller and Y. Aloimonos. Ambiguity in structure from motion: Sphere versus plane. *International Journal of Computer Vision*, 28:137–154, 1998.

[6] Christopher Geyer and Kostas Daniilidis. Structure and motion from uncalibrated catadioptric views. In *Proc. IEEE Conference on Computer Vision and Pattern Recognition*, 2001.

[7] Micheal D Grossberg and Shree Nayar. A general imaging model and a method for finding its parameters. In *Proc. International Conference on Computer Vision*, volume II, pages 108–115, 2001.

[8] Rajiv Gupta and Richard Hartley. Linear pushbroom cameras. *IEEE Transactions on Pattern Analysis and Machine Intelligence*, 19(9):963–975, 1997.

[9] Richard Hartley and Andrew Zisserman. *Multiple View Geometry*. Cambridge University Press, 1999.

[10] N Justin Marshall and Michael F Land. Some optical features of the eyes of stomatopods: I. Eye shape, optical axes and resolution. *Journal of Comparitive Physiology, A*, 173:565–582, 1993.

[11] Randall Nelson and John Aloimonos. Finding motion parameters from spherical flow fields (or the advantage of having eyes in the back of your head). *Biological Cybernetics*, 58:261–273, 1988.

[12] Tomas Pajdla. Characterization of epipolar geometries of non-classical cameras. Technical Report CTU-CMP-2001-05, Czech Technical University in Prague, December 2001.

[13] Shmuel Peleg, Yael Pritch, and Moshe Ben-Ezra. Cameras for stereo panoramic imaging. In *CVPR*, pages 208–214, 2000.

[14] J. Plücker. On a new geometry of space. *Philisophical Transactions of the Royal Society of London*, 155:725–791, 1865.

[15] Paul Rademacher and Gary Bishop. Multiple-center-of-projection images. In *SIGGRAPH*, 1998.

[16] Zhengyou Zhang. A flexible new technique for camera calibration. *IEEE Transactions on Pattern Analysis and Machine Intelligence*, 22(11):1330–1334, 2000.